Borohydride and metallic copper as a robust dehalogenation system: Selectivity assessment and system optimization

Ali Shee, Frank-Dieter Kopinke and Katrin Mackenzie*

Helmholtz Centre for Environmental Research-UFZ, Department of Environmental Engineering

Permoserstraße 15, D-04318 Leipzig, Germany

*Correspondence:

Email: katrin.mackenzie@ufz.de

Abstract

Hydrodechlorination (HDC) using noble-metal catalysts in the presence of H-donors is a promising tool for the treatment of water contaminated by halogenated organic compounds (HOCs). Cu is an attractive alternative catalyst to noble metals since it is cheaper than Pd, Rh, or Pt and more stable against deactivation. Cu with borohydride (BH_4^-) as reductant (copper-borohydride reduction system; CBRS) was applied here for the treatment of saturated aliphatic HOCs. The HDC ability of CBRS was evaluated based upon product selectivities during reduction of CCl_3–R compounds (R = H, F, Cl, Br, and CH_3). For $CHCl_3$, CH_2Cl_2, and $CHCl_2$–CH_3, the dechlorination reaction proceeds predominantly via α-elimination with initial product selectivities to CH_4 and C_2H_6 of 84-85 mol-% and 70-72 mol-%. For CCl_4, $CBrCl_3$, $CFCl_3$, and CCl_3–CH_3, stepwise hydrogenolysis dominates. CH_2Cl–R compounds are formed as recalcitrant intermediates with initial selectivities of 50-72 mol-%, whereas CH_4 and C_2H_6 are minor products with 16-35 mol-% and 30-35 mol-%. The effect of reaction conditions on product selectivities were investigated for $CHCl_3$ as target. Solution composition, variation of reducing agents (BH_4^-, H* from H_2) and increase of electron pressure (electric potential at Cu electrode and Fe^0 as support) did not have marked influence on the selectivities (ratio of CH_4:CH_2Cl_2). Product selectivities for

reduction of CCl_3–R compounds were found to be substrate-specific rather than reductant-specific. Since the formation of halogenated by-products could not be avoided, transformation via a second reduction step was optimized by higher catalyst dose, addition of Ag, and vitamin B12 to the CBRS. Comparison between Pd and Cu based on costs, catalyst activities, selectivities, metal stability, and fate of halogenated by-products shows that the CBRS is a potent alternative to conventional HDC catalysts and can be recommended as 'agent of choice' for treatment of α-substituted haloalkanes in heavily contaminated waters.

Keywords: Copper catalysts, borohydride, halogenated organic compounds, reduction processes, product selectivity patterns.

Introduction

Chemical reduction of halogenated organic compounds (HOCs) in aqueous media is a common and convenient means for detoxification of contaminated water. This is achieved through selective removal of the halogen atoms (R–X + reducing agent → R–H + X^-) with a minimal requirement of redox equivalents. Although sometimes less-halogenated intermediates may remain, coupling chemical reduction with biological methods can achieve the desired clean-up performance (Dong et al., 2019; Vogel et al., 2018). Saturated aliphatic compounds with the general formula CCl_3–R, including chloroform (CF), carbon tetrachloride (CTC), trichlorofluoromethane ($CFCl_3$), bromotrichloromethane ($CBrCl_3$), and 1,1,1-trichloroethane (1,1,1-TCA), are pollutants of interest for environmental catalysis. Hydrodehalogenation of these CCl_3–R compounds to produce the fully dehalogenated products, CH_4 and C_2H_6, is desirable. Partial dehalogenation to halogenated by-products such as dichloromethane (DCM),

monochloroethane (MCA), and substances with intact C–F bond that remain in the system more or less as dead-end products, are undesired in a water treatment technology.

An evaluation of the literature shows that the product patterns during the reduction of saturated aliphatic chlorohydrocarbons in water vary greatly depending upon which reductants and catalysts are applied. After application of zero-valent iron (ZVI) and other Fe-based materials (e.g. Fe_2O_3) for dechlorination of saturated chloroaliphatics, significant amounts of chlorinated by-products remain (Balko and Tratnyek, 1998; Danielsen et al., 2005; Elsner et al., 2004; Fennelly and Roberts, 1998; Li and Farrell, 2000; McCormick, 2002; McCormick and Adriaens, 2004; Song and Carraway, 2006; Song and Carraway, 2005). As an alternative to ZVI, platinum-group catalysts (Pd, Rh, Pt) generate fewer chlorinated by-products. Among the platinum group catalysts, Pd is most widely applied due to its high catalytic activity. Pd is rather resistant in water against self-poisoning by halide (X^-) especially in the presence of bases, e.g. NaOH (Benitez and Del Angel, 2000; Urbano and Marinas, 2001). The hydrodechlorination (HDC) of CTC and CF at Pd surfaces produces CH_4 as the major product and only traces of chlorinated by-products (Lowry and Reinhard, 1999; Ordóñez et al., 2000; Velázquez et al., 2013; Wang et al., 2009). Nevertheless, monochloromethane (MCM) and DCM persist more-or-less as dead-end products. Therefore, a treatment system that can minimize the accumulation of such slowly reacting and toxic chlorinated by-products under mild reaction conditions will be a better alternative to Pd and other platinum-group catalysts.

In the current study, Cu catalysts in combination with borohydride (BH_4^-) as reductant were investigated for the dehalogenation of saturated aliphatic HOCs. Cu is much cheaper than the Pt-group metals and is readily available on the world market. For example, one gram of Pd costs about USD 80 (Palladium Prices, 2021) while one gram of Cu costs approximately USD 0.009

(Copper Prices, 2021), meaning that Cu is cheaper by about four orders of magnitude than Pd. Furthermore, Cu is moderately tolerant against deactivation by common catalyst poisons, including sulfite and sulfide, whereas Pt-group metals suffer from total and permanent deactivation of the catalysts whereby full regeneration is hard to achieve (Angeles-Wedler et al., 2008; Angeles-Wedler et al., 2009; Han et al., 2016; Lim and Zhu, 2008; Lowry and Reinhard, 2000). Cu is not able to utilize molecular hydrogen (H_2) in HDC reactions. However, metallic copper in combination with the strong reductant borohydride, herein referred to as copper-borohydride reduction system (CBRS), is a potent reduction system. The CBRS has also been demonstrated to dechlorinate DCM (Huang et al., 2012) and 1,2-DCA (Huang et al., 2011) at reasonable rates. These substances resist reduction by ZVI and Pd + H_2. The objective of this study was a deeper insight into the performance of the CBRS, based upon the evaluation of a potential application in the treatment of saturated aliphatic HOCs, in order to provide information regarding: i) product patterns from compounds with the general formula CCl_3–R, ii) the influence of reaction conditions on the product patterns, and iii) the optimal reaction conditions for treatment of the target contaminants.

Experimental Section

Chemicals and reagents

All chemicals and reagents used were of the highest analytical grade available. They were used as received without further purification. The names and suppliers of the various chemicals and reagents are provided in the Supporting Information (SI) section in TABLE SI 1.

Preparation of Cu, Pd, and nZVI nanoparticles

Cu nanoparticles (Cu NPs) were synthesized using a protocol similar to that described elsewhere (Huang et al., 2011). Typically, the pH value of a 60 mL aqueous solution of $CuSO_4 \cdot 5H_2O$ (c_{Cu} = 100 mg/L) was adjusted to 10 using 1 M NaOH to form $Cu(OH)_2$ as an intermediate. The solution was then deoxygenated by purging with nitrogen followed by the addition of an aqueous solution of $NaBH_4$ ($c_{0,NaBH4}$ = 300 mg/L) to produce the Cu NPs. The Cu NPs prepared by this technique had mean particle size d_{50} = 50 nm as determined by nanoparticle tracking using NanoSight LM10 and NTA 2.0 Analytical Software. The Brunauer-Emmett-Teller (BET) surface area as determined by means of N_2-adsorption-desorption measurements for Cu NPs was 15 m^2/g.

Palladium nanoparticles (Pd NPs) were synthesized from aqueous palladium (II) acetate by adapting a similar procedure reported elsewhere (Hildebrand et al., 2009). An aqueous solution of the Pd salt solution was flushed with hydrogen for 60 min. The Pd NPs were isolated from the aqueous suspension by centrifugation and the mean particle size of the nanoparticles was d_{50} = 60 nm as determined by NTA analysis.

nZVI particles were generated by reduction of an aqueous solution of $FeSO_4 \cdot 7H_2O$ using $NaBH_4$ adapting a procedure described elsewhere (Feng and Lim, 2007). The nZVI particles were isolated from the aqueous media by centrifugation, and the excess borohydride was removed by several washing steps with oxygen-free water. The nZVI particles had a mean size d_{50} = 75 nm as determined by NTA analysis and were in the size range of 50 to 100 nm.

Dehalogenation experiments

Batch experiments were carried out in 120 mL serum bottles sealed with Teflon™-lined butyl rubber septa and aluminum crimp caps. 20 mL headspace was applied for CTC, CFC-11 while 60 mL headspace was used for CF, DCM, 1,1-DCA, and 1,1,1-TCA. For each dehalogenation experiment, freshly prepared Cu NPs (c_{Cu} = 0.2-100 mg/L) were applied with $NaBH_4$ ($c_{0,NaBH4}$ = 300 mg/L) as the reductant. The Cu NPs were applied as prepared without their separation from the aqueous phase. The aqueous suspension was deoxygenated by purging with nitrogen followed by spiking a methanolic solution of the educt into the suspension in order to initiate the dehalogenation reaction (t = 0). The batch reactors were shaken horizontally at 130 rpm. Control experiments were performed using either Cu NPs or $NaBH_4$ in separate experiments under identical conditions.

Analytical techniques

Standard aqueous solutions of the test substances were used to prepare calibration curves. Analysis of the educts and products was done by gas chromatography coupled with mass spectrometry (GCMS-QP2010, Shimadzu). The GC was equipped with a DB-1ms capillary column (J & W, 60 m x 0.25 mm x 0.25 µm). The temperature conditions for the injector port, column oven, interface, and detector were set to 180, 40, 200, and 250 °C, respectively. At each sampling time, 25 µL of the headspace was extracted using a gastight syringe and injected into the GC. The split ratio for the GC was set to 5. Methane (CH_4), ethane (C_2H_6), and ethene (C_2H_4) were quantified by means of a GC (GC 2010 Plus, Shimadzu) equipped with a wide bore column (GS-Q, 30 m x 0.53 mm x 1.00 µm) and flame ionization detector (FID). The temperature conditions for the GC were set to 200, 40, and 280 °C for the injector, column oven, and detector, respectively.

Similarly, a 25 µL gastight glass syringe was used for headspace hydrocarbon sampling for GC analysis. The GC split ratio was set to 5. The concentration of educt and each product was determined by the external standard method using calibration curves. Since the decomposition of $NaBH_4$ in water leads to H_2 production during the course of the reaction, resulting in an expanded headspace volume, propane and to some extent methyl tert-butyl ether were used as internal standards. Raw experimental data were corrected based upon the internal standard peak areas at each sampling point. Chloride, bromide, and fluoride were analyzed via ion chromatography (IC) (IC25, Dionex, IonPac AS15/AG15). 1 mL aliquots were extracted from the batch reactor and filtered through a filter membrane (0.45 µm) before injection into the IC.

In order to determine the efficiency of the dehalogenation reaction, the product yields and selectivities were calculated according to equations 1 and 2, respectively:

$$Y_{\mathrm{i,product}} = \frac{n_{\mathrm{i,product}}}{n_{\mathrm{HOC,0}}} \times 100\ \% \tag{1}$$

$$S_{\mathrm{i,product}} = \frac{n_{\mathrm{i,product}}}{n_{\mathrm{converted\ HOC}}} \times 100\ \% \tag{2}$$

where $Y_{\mathrm{i,product}}$ is the yield of a given product i (mol-%), $n_{\mathrm{i,product}}$ refers to the moles of product i obtained at a given time (mol), and $n_{\mathrm{HOC,0}}$ refers to the moles of educt fed into the reactor at time $t = 0$ (mol). For equation 2, $S_{\mathrm{i,product}}$ is the selectivity to a given product i (mol-%) and $n_{\mathrm{converted\ HOC}}$ refers to the moles of educt converted at the given time (mol).

In order to evaluate the reaction rates of the HOCs during the dehalogenation reaction, the specific metal activity (A_{m}) was applied as a rate parameter. A_{m} is equivalent to a second-order rate constant derived from the observed first-order rate constant k_{obs}. In cases where clear first-order

kinetics cannot be observed, A_m is approximated from the first half-life $\tau_{½}$ of the educt. A_m was calculated based upon equation 3:

$$A_{\mathrm{m}} = \frac{V_{\mathrm{w}}}{m \cdot \tau_{½}} = \frac{1}{c_{\mathrm{m}} \cdot \tau_{½}} = \frac{k_{\mathrm{obs}}}{In\, 2 \cdot c_{\mathrm{m}}} \qquad [\mathrm{L/(g{\cdot}min)}] \qquad (3)$$

where V_w is the volume of contaminated water (L), m is the metal mass (g), $\tau_{½}$ is the HOCs half-life (min) obtained from the dehalogenation profile of the test substance and c_m is the metal concentration (g/L).

Results and Discussions

Product selectivity patterns during the dechlorination of chloroform

CF is a prominent member of the group of saturated aliphatic chlorinated compounds, is commonly found as a disinfection by-product in water and is therefore an important target of environmental catalysis. CF was selected in the present study as a probe compound in order to gain relevant information regarding product selectivity patterns. Reductive dechlorination of CF by Pd + H_2 and ZVI is characterized by low reaction rates and formation of DCM and MCM as dead-end by-products (Mackenzie et al., 2006; Song and Carraway, 2006). As can be seen in FIGURE 1, CF is readily transformed by the CBRS.

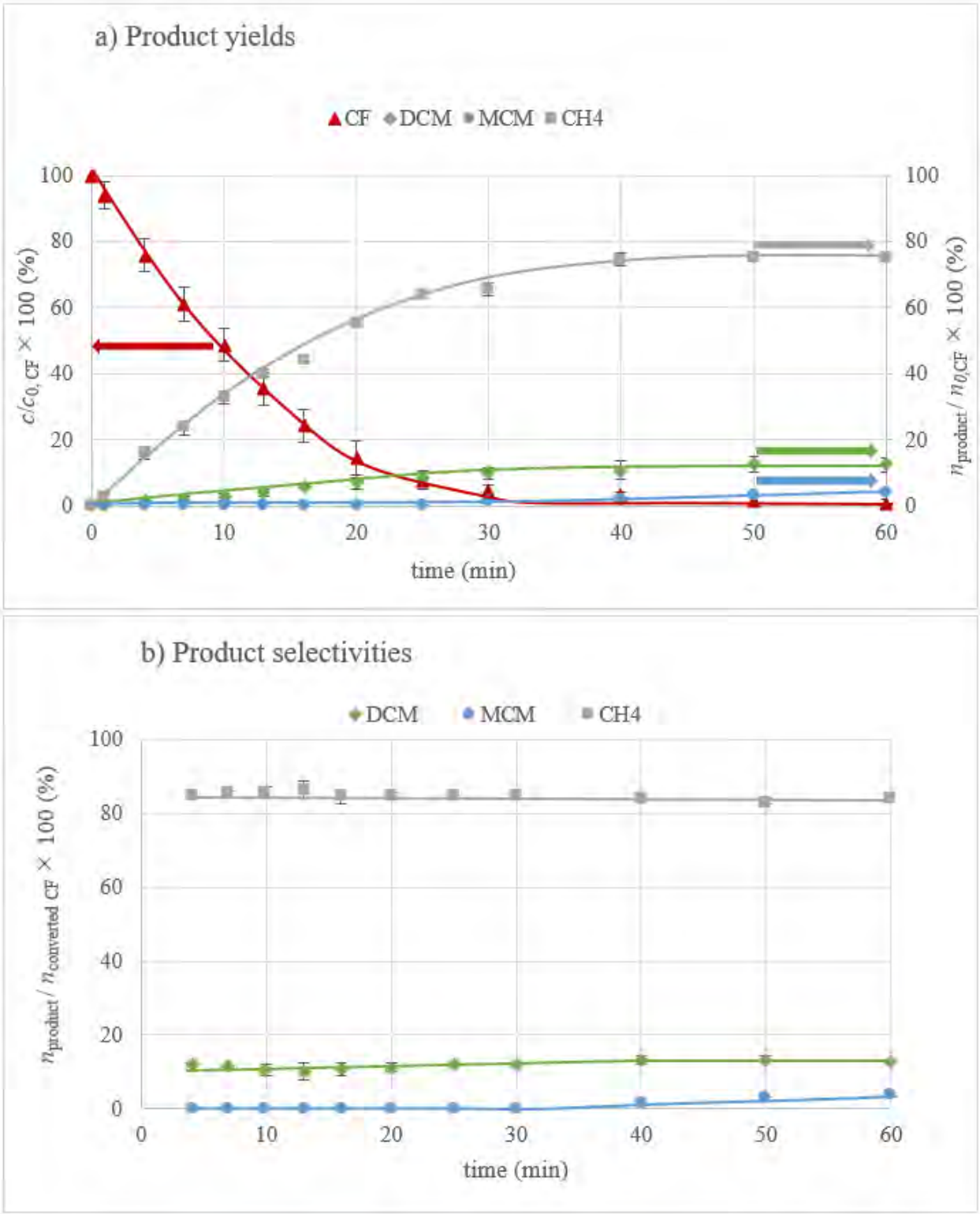

FIGURE 1. Reaction progress during the dechlorination of CF in water by CBRS: a) product yields and b) product selectivities (c_{Cu} = 1 mg/L; $c_{0,NaBH4}$ = 300 mg/L; $c_{0,CF}$ = 10 mg/L;

pH = 10). Note that for MCM, the values in both graphs are multiplied by a factor of 20. The limit of detection for MCM using GCMS under SIM mode was 0.001 mg/L.

In FIGURE 1 (a), it can be seen that from the beginning of the dechlorination reaction, CH_4, DCM, and MCM are produced as primary products. At t = 40 min, where the CF conversion was ≥ 95 %, the products yields were divided into (76 ± 1) mol-%, (12 ± 1) mol-%, and (0.5 ± 0.2) mol-% for CH_4, DCM, and MCM, respectively. The scattering ranges result from three parallel experiments. FIGURE 1 (b) shows product partitioning in the course of the dechlorination reaction. At t = 4 min, as can be seen in FIGURE 1 (b), the selectivities to MCM, DCM, and CH_4 were (0.3 ± 0.2) mol-%, (13 ± 2) mol-%, and (84 ± 2) mol-%, respectively. These selectivities were nearly constant over the entire CF conversion range. Therefore, the CF dechlorination reaction can be described by three main parallel pathways forming the various products, and consecutive reaction pathways play only a minor role within this time window. Other products detected were C_2H_6 and C_2H_4, which accounted for < 0.5 mol-% of CF converted. The Cl^- yield at t = 60 min was (80 ± 2) mol-%, which conforms to the chlorine amounts released from the detected products (76 % + 12 % × 1/3 + 0.5 % × 2/3 = 80.0 mol-%). The detection of small amounts of C_2-hydrocarbons is an indication that radical coupling reactions do not take place but play only a minor role. In similar studies for the dechlorination of CF and CTC, the radical coupling products C_2H_6, PCE, and TCE were also reported (Feng and Lim, 2007; McCormick and Adriaens, 2004; Velázquez et al., 2013). In the present study, TCE and PCE were not detected. Considering both the chlorine and carbon balances, a fraction of about 11.5 mol-% of non-detected (non-identified) chlorinated reaction products remains. Part of the balance gap may be due to gas-phase losses, due to hydrogen gas formation from borohydride, despite the internal standard application.

For evaluation of kinetic data, the decomposition rate of $NaBH_4$ may become significant. $NaBH_4$ is readily hydrolyzed in water ($NaBH_4 + 2H_2O \rightarrow NaBO_2 + 4H_2$) and the decomposition rate is pH sensitive ($BH_4^- + H^+ + 3H_2O \rightarrow 4H_2 + H_3BO_3$) (Liu and Li, 2009; Retnamma et al., 2011). For example, the half-life for decomposition of $NaBH_4$ at pH 6.5 is 7 s (Wade, 1983). In order to control the decomposition of $NaBH_4$, the experimental conditions had to be adjusted. In this study, the half-life for decomposition of $NaBH_4$ at pH 10 and c_{Cu} = 1 mg/L was about 10-12 h. Hence, the BH_4^- concentration under the reaction conditions can be considered constant during the CF dechlorination time window. Based on the products detected as shown in FIGURE 1, the possible reaction pathways for the dechlorination of CF using CBRS are presented in FIGURE 2.

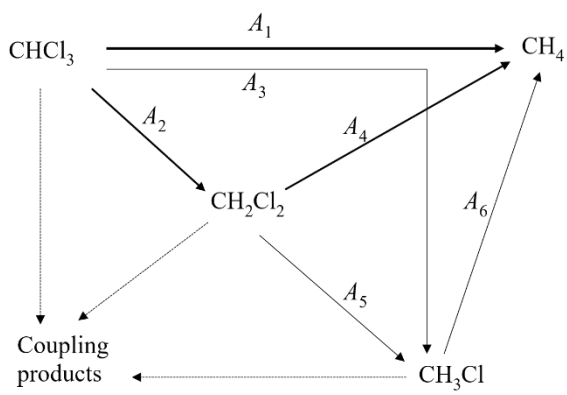

FIGURE 2. Proposed reaction pathways for the dechlorination of CF in water using CBRS. (c_{Cu} = 1-100 mg/L; $c_{0,NaBH4}$ = 300 mg/L; $c_{0,HOCs}$ = 2-10 mg/L; pH = 10). The reaction scheme is based on the product selectivity pattern in FIGURE 1 (b).

Using additional experiments presented later in this chapter, the specific Cu activities A_{Cu} for the expected by-products were determined by using them as educts in separate dechlorination tests under H_2 gas phase. The specific copper activities are presented in TABLE 1.

TABLE 1. Specific Cu activities A_{Cu} for the dechlorination of CF, DCM, and MCM using CBRS according to FIGURE 2 from educts (c_{Cu} = 1-100 mg/L; $c_{0,NaBH4}$ = 300 mg/L; p_{H2} = 100 kPa; pH = 10).

Specific Cu activity A_{Cu} [L/(g·min)]	A_{CF}	A_1	A_2	A_3	A_{DCM}	A_4	A_5	A_6
	130 ± 10[a]	110 ± 5[b]	17 ± 5[b]	0.6 ± 0.2[b]	0.22 ± 0.02[c]	0.19 ± 0.01[d]	0.029 ± 0.002[d]	0.0020 ± 0.0002[e]

[a] A_{CF} represents the overall specific Cu activity for the dechlorination of CF.
[b] Value calculated from CF as the educt.
[c] A_{DCM} represents the overall specific Cu activity for dechlorination of DCM.
[d] Value calculated from experiments with DCM as educt.
[e] Value calculated from experiments with MCM as educt.

In order to determine whether DCM and MCM are 'free' intermediates on the pathway from CF to CH_4, separate experiments were done for the dechlorination of DCM and MCM using CBRS under reaction conditions similar to those applied for CF. As shown in TABLE 1, these resulted in $A_{Cu,DCM}$ = (0.22 ± 0.02) L/(g·min) and $A_{Cu,MCM}$ = (0.0020 ± 0.0002) L/(g·min). Therefore, CH_4 is formed directly from CF, not through stepwise hydrogenolysis via DCM and MCM. Hence, reactions **4**, **5,** and **6** do not significantly contribute to the overall dechlorination during the CF conversion. We surmise the dechlorination of CF through the α-elimination (-HCl) pathways via dichlorocarbene intermediates (:CCl_2), as this may account for the formation of CH_4 (McCormick and Adriaens, 2004; Song and Carraway, 2006). Based on the product patterns (FIGURE 1), three main parallel reactions **1**, **2,** and **3** (FIGURE 2) can be applied in order to describe the dechlorination of CF by CBRS. The complete dechlorination reaction **1** leading to CH_4 is to be preferred in water-treatment applications. The partial dechlorination reactions **2** and **3** leading to DCM and MCM, respectively, are undesired. Both DCM and MCM persist even after the CF dechlorination reaction shown in FIGURE 1 was continued for 20 h ($c_{20h,NaBH4}$ = 75 mg/L). Hence, they can be considered more-or-less as dead-end products under the experimental conditions (c_{Cu} = 1 mg/L). From a remediation perspective, the accumulation of partially dechlorinated products (which in most cases are toxic) is highly undesired. In this study, DCM

was the major undesired by-product and is a water contaminant of public health concern due to its carcinogenic potential (Dekant et al., 2021; Schlosser et al., 2015). Further studies were performed in order to minimize DCM formation under different experimental conditions. FIGURE 3 shows apparent product selectivities using Cu NP concentrations in the range c_{Cu} = 0.1 to 100 mg/L and $c_{0,NaBH4}$ = 300 mg/L.

FIGURE 3. Effect of Cu NPs concentration on the apparent product selectivities during the dechlorination of CF ($c_{0,NaBH4}$ = 300 mg/L; $c_{0,CF}$ = 10 mg/L; pH = 10). Selectivity patterns were determined at the termination of reaction after 60 min where CF conversion was ≥ 95 %.

Using low catalyst concentrations in the range of 0.1 to 0.5 mg/L (FIGURE 3), product patterns were more-or-less similar. The 'apparent' DCM selectivity decreases at elevated catalyst amounts. At the maximal catalyst concentration (c_{Cu} = 100 mg/L), 'apparent' selectivities to CH_4 and DCM were (98 ± 1) mol-% and (0.5 ± 0.2) mol-%, respectively. These are not primary product selectivities ($S_{i,product}$ for CF conversion) but are affected by subsequent DCM dechlorination. Nevertheless, an approximation of the DCM half-life from the activity data in TABLE 1 shows

that even in the presence of 100 mg/L Cu catalyst, the DCM should be relatively long-living: $\tau_{½} = 1/(A_{Cu} \cdot c_{Cu}) = 1/(0.2\ L/(g\ min) \cdot 0.1\ (g/L)) = 50$ min. This means that the specific catalyst activity or/and its selectivity is also affected by its concentration. It may be explained by the nanoparticulate state of the suspended Cu catalyst. Although this approach prevents the accumulation of DCM, it comes at the expense of a much higher catalyst concentration, with consequences for a technical application.

Comparison of Cu-, Pd- and nZVI-based systems for dechlorination of CF

From the data on dechlorination of CF using the CBRS, it can be seen that there are parallel reaction pathways to CH_4, DCM, and MCM. Therefore, we pose the question: what is the role of borohydride as the reducing agent in this selectivity pattern? In order to answer this question, the dechlorination of CF in water and under ambient conditions was further investigated using Pd + H_2, Pd + BH_4^-, and nZVI (TABLE 2).

TABLE 2. Selectivity patterns during the dechlorination of CF in water using Cu + BH_4^-, Pd + BH_4^-, Pd + H_2, and nZVI under ambient conditions (c_{Cu} = 1 mg/L; c_{Pd} = 3-5 mg/L; $c_{0,NaBH4}$ = 300 mg/L; c_{nZVI} = 5 g/L).

Reduction system	$n_{product} / n_{converted\ CF} \times 100$ (%)			**Specific metal activities A_m L/(g·min)**	**Cl^- yield (mol-%)**
	CH_4	**DCM**	**MCM**		
Cu + BH_4^- (this study)	84 ± 2	13 ± 2	0.3 ± 0.2	130 ± 10	80 ± 2
Pd + BH_4^- (this study)	78 ± 4	15 ± 3	5 ± 2	10 ± 2	75 ± 3
Pd + H_2 (this study)	80 ± 3	11 ± 2	8 ± 2	5 ± 1	78 ± 3
Pd/Al_2O_3 + H_2 (Velázquez et al., 2013)	90	10	n.a.	n.a.	n.a.
PdAu/Al_2O_3 + H_2 (Velázquez et al., 2013)	94.4	5.5	0.1	n.a.	n.a.
Pd/Al_2O_3 + H_2 (Lowry and Reinhard, 1999)	80	n.a.	n.a.	n.a.	n.a.
nZVI (this study)	24 ± 2	40 ± 5	35 ± 5	0.003 ± 0.001	50 ± 5

n.a. = not analyzed

Selectivities were calculated at 25-35 % CF conversion; pH_0 for nZVI was 8.3 which increased to 9 at the termination of the reaction. No BH_4^- or H_2 was added into the reactor during CF dechlorination by nZVI; pH for the systems Pd + BH_4^-, Pd + H_2, and Cu + BH_4^- remains about 10. Chloride yield measured at termination of reaction where CF conversion was ≥ 95 %. Selectivities for the systems Pd/Al_2O_3 + H_2 and $PdAu/Al_2O_3$ + H_2 were obtained from literature. For the remediation systems which were tested in this study, the sum of C_2H_6 and C_2H_4 accounts for 0.5-2 mol-% of CF converted. The specific metal activities A_m were calculated using nanoparticles of comparable sizes, i.e. $d_{50,\text{Cu NPs}}$ = 50 nm, $d_{50,\text{ Pd NPs}}$ = 60 nm and $d_{50,\text{nZVI}}$ = 75 nm (particle sizes are presented in TABLE SI 2).

The synthesis of nZVI was done by reduction of $FeSO_4 \cdot 7H_2O$ using borohydride, adapting a procedure described elsewhere (Feng and Lim, 2007). Pd nanoparticles were prepared by reduction of an aqueous solution of Pd (II) acetate with hydrogen using a procedure similar to that reported elsewhere (Hildebrand et al., 2009). Based on literature data and own experimental results, the product selectivity patterns during the dechlorination of CF using Cu-, Pd- and nZVI-based systems are shown in TABLE 2. When comparing the dechlorination abilities of Cu-, Pd- and nZVI-based systems, one has to take into account that different 'reduction systems' are compared rather than metals because each of the three systems uses its own reductant (BH_4^-, H_2, and Fe^0, respectively). Metallic Cu and Pd are true catalysts: in the presence of a reductant, the dechlorination process may involve the transfer of H-species (active H*) in the form of either chemisorbed H-atoms or hydrides. nZVI, however, is a reagent, whereby some catalytic properties are possible. As shown in TABLE 2, the selectivity to CH_4, DCM, and MCM during the dechlorination of CF changes depending upon which catalyst or reagent was used. Since CH_4, DCM and MCM selectivities were nearly the same using the systems CBRS, Pd + H_2, Pd + BH_4^-, and Pd/Al_2O_3 + H_2, one can speculate that the dechlorination reaction follows a similar mechanism, despite the quite different catalysts and reductants ($NaBH_4$ or H_2). As shown in FIGURE SI 1, the initial reductant concentration ($c_{0,\text{NaBH4}}$ = 25-500 mg/L) supplied had no marked effect on product patterns under standard reaction conditions (pH = 10, $c_{0,\text{CF}}$ = 10 mg/L and c_{Cu} = 1 mg/L). For the Pd-based catalysts, the type of reductants ($NaBH_4$ or H_2) has no marked

effect on selectivities. As shown in TABLE 2, the specific Pd activities A_{Pd} for the dechlorination of CF using Pd + H_2 and Pd + BH_4^- were (5 ± 1) L/(g·min) and (10 ± 2) L/(g·min), respectively. This difference in Pd activities is rather small, indicating that $NaBH_4$ plays the role of a hydrogen source only, rather than participating directly in the dechlorination reaction. DCM selectivity was lower by a factor of 2 for PdAu/Al_2O_3 + H_2 than for Pd/Al_2O_3 + H_2 systems. As will be discussed later, Ag, which is in the same group as Au in the periodic table, has a marked effect in decreasing DCM selectivities. This implies that the choice of metal or metal combinations may be an appropriate tool for achieving the desired low selectivity towards DCM. Since the selectivities were nearly the same for Pd/Al_2O_3 + H_2, Pd + H_2, and Pd + BH_4^-, one can conclude that borohydride as a reductant has no marked influence on the product selectivities. Remarkably, Pd favors the formation of MCM much more than Cu (by a factor of 17), which might be due to the higher availability of active H* at the Pd surface, necessary for stepwise hydrogenolysis of chemisorbed intermediates. Mackenzie et al. (2006) have determined specific Pd activities A_{Pd} for HDC of various chlorinated hydrocarbons in water, among them CF and DCM, under identical reaction conditions with Pd/γ-Al_2O_3 + H_2. The obtained values $A_{Pd,CF}$ = 0.8 L/(g·min) and $A_{Pd,DCM}$ = 0.0015 L/(g·min) yield a ratio $A_{Pd,CF}/A_{Pd,DCM}$ = 530. For CBRS, the corresponding ratio is $A_{Cu,CF}/A_{Cu,DCM}$ = 590 (data from TABLE 1). Surprisingly, the two ratios are quite similar despite the different catalysts and reductants applied. This may be a coincidence or an indication of similar initial rate-controlling steps. From the remediation point of view, it means that Pd + H_2 and CBRS both have similar problems in principle concerning the formation of DCM during the dechlorination of CF. However, whereas DCM remains as a recalcitrant by-product for Pd systems, DCM is not a problem for CBRS when using higher Cu amounts. Copper is by far the cheaper metal (cheaper than Pd by a factor of 8500), but $NaBH_4$ compared to H_2 is the more expensive

reductant, and the aqueous suspension must be alkaline. As can be seen in TABLE 2, nZVI as an electron-transmitting reagent is not useful for dechlorination of CF due to the higher selectivities to chlorinated by-products. From TABLE 2, the selectivities to CH_4, DCM, and MCM were (24 ± 2) mol-%, (40 ± 5) mol-%, and (35 ± 5) mol-%, respectively. Both DCM and MCM are stable to transformation using nZVI, and hence remain as dead-end by-products. Comparison of CBRS, Pd + H_2, and nZVI based upon the specific metal activities for dechlorination of CF (data in TABLE 2) shows that $A_{\mathrm{Cu,CF}}$ is the highest by two and five orders of magnitude compared to $A_{\mathrm{Pd,CF}}$, and $A_{\mathrm{nZVI,CF}}$, respectively. Although alkaline conditions (pH = 10) are necessary in order to control the rate of $NaBH_4$ decomposition in water, CBRS is by far the most potent HDC system compared to the common HDC systems e.g. Pd + H_2, taking into consideration specific metal activities, the ability for dechlorination of DCM and MCM, metal cost and metal stability. Nevertheless, adjusting the pH of the treated effluent from 10 to 6-8 will presumably be necessary before discharge into the environment.

Effect of reaction conditions on product selectivity patterns during the dechlorination of CF

In general, product selectivity patterns may differ greatly when reactions are carried out in the presence of background electrolytes commonly present in natural waters. In order to test this for the CBRS, NaF, NaCl, KBr, SRHA, Na_2SO_3, Na_2SO_4, $NaHCO_3$, $MgSO_4$, $CaCl_2$, $MnSO_4$, $FeSO_4$, $NaNO_3$, $NaNO_2$, and Na_2S were supplied. Except for Na_2S (FIGURE SI 2), all these co-solutes (10 mg/L) had only negligible effects on the DCM selectivity patterns. Na_2S was present under the experimental conditions (pH = 10) as bisulfide (HS^-, pK_a = 12.9). The strong interaction of HS^- with Cu modifies the catalyst surface (partial formation of CuS). Due to this modification, selectivities to CH_4, DCM, and MCM under the applied conditions were (60 ± 5) mol-%, (24 ± 2) mol-%, and (12 ± 2) mol-%, respectively. The DCM and MCM selectivities were higher

by factors of 2 and 40, respectively, compared to the baseline for clean Cu^0. Hence, prevention of Cu deactivation by sulfur species may be necessary for optimal performance. However, re-reduction of the Cu surface by borohydride could take place in parallel to sulfidation (see FIGURE SI 3).

Next, multimetal catalysts comprising Cu/Zn, Cu/Ce, Cu/Al, Cu/Sn, and Cu/Co were prepared by reduction of mixtures of metal ions in the same batch reactor with $NaBH_4$. The speciation of the metals in the resulting particles (separate particles, coatings, or alloys) was not analyzed. For all these multimetal catalysts, a slight increase in DCM selectivity (FIGURE SI 4) was observed compared to the monometallic Cu NPs. This shift was combined with a gradual loss of catalyst activity (FIGURE SI 5). A significant change in selectivities was obtained when CF dechlorination was carried out using Ag (c_{Ag} = 2 mg/L) + BH_4^- and Ag/Cu (c_{Ag} = 0.5 mg/L and c_{Cu} = 1.5 mg/L) + BH_4^-. For all Ag-containing catalysts, the primary selectivities to CH_4, DCM, and MCM were 90-92, 2-3, and 5-6 mol-%, respectively. The DCM selectivity was lower by a factor of 6.5 than the baseline for pure Cu NPs ($S_{Cu,DCM}$ = (13 ± 2) mol-%), but the MCM selectivity was higher by a factor of 17. With all Ag-containing catalysts, MCM remained as a dead-end by-product. DCM does not accumulate but is subsequently dechlorinated. The specific activities for dechlorination of DCM using Ag and Ag/Cu were $A_{Ag,DCM}$ = (2.1 ± 0.5) L/(g·min) and $A_{Ag/Cu,DCM}$ = (1.0 ± 0.5) L/(g·min), respectively. These activities were 9.5 and 4.5 times higher for Ag and Ag/Cu, respectively, compared to the baseline for pure Cu. The specific activity of pure Ag NPs for dechlorination of CF was $A_{Ag,CF}$ = (20 ± 5) L/(g·min), which is lower by a factor of 6.5 than the baseline activity for pure Cu NPs ($A_{Cu,CF}$ = (130 ± 10) L/(g·min)) and a factor of 4 lower than that of the mixed Ag/Cu NPs ($A_{Ag/Cu,CF}$ = (80 ± 5) L/(g·min)). The ratio of activities for dechlorination of CF and DCM is $A_{Ag,CF}/A_{Ag,DCM}$ = 9.5 and $A_{Ag/Cu,CF}/A_{Ag/Cu,DCM}$ = 80 for Ag and

Ag/Cu, respectively. Considering the activity ratios $A_{Cu,CF}/A_{Cu,DCM}$ = 590 and $A_{Pd,CF}/A_{Pd,DCM}$ = 530, it becomes obvious that Ag-containing catalysts can better handle the DCM issue. Ag-doped Cu is recommended for dechlorination of CF. However, it cannot be disregarded that MCM selectivities are an order of magnitude higher with Ag-containing catalysts (5 mol-% compared to 0.3 mol-% with pure Cu). In the frame of the reaction scheme in FIGURE 2, this points to a faster reaction pathway with the reactions (2) and (5), whereas reaction (6) is not accelerated. In addition, Ag is more expensive than Cu by a factor of about 90 (about USD 0.84/g Ag) (Silver Prices, 2021) versus USD 0.009/g Cu).

Huang et al. have found that vitamin B12 (with its Co center) can accelerate the Cu-catalyzed dechlorination of DCM (Huang et al., 2013; Huang et al., 2015). Based on this finding, CBRS + vitamin B12 was tested for dechlorination of CF. This combination decreased the apparent selectivity towards DCM from (13 ± 2) mol-% for pure Cu to (2 ± 1) mol-%. This was due to the further dechlorination of DCM and therefore it is not a 'true' selectivity effect. The specific metal activity ($A_{m,DCM}$ = (15 ± 3) L/(g·min)) was higher by a factor of 70 than for pure Cu ($A_{Cu,DCM}$ = (0.22 ± 0.02) L/(g·min)). MCM selectivity was (3 ± 1) mol-% which was higher by a factor of 10 than for Cu (S_{MCM} = (0.3 ± 0.2) mol-%). Nevertheless, MCM was not a dead-end product but was subsequently dechlorinated when the reaction was continued for 120 min. Also, CBRS + vitamin B12 was more potent for the dechlorination of CF, resulting in $A_{Cu/vB12,CF}$ = (260 ± 20) L/(g·min)), which is higher by a factor of 2 than for pure Cu. When Cu/Co + BH_4^- and vitamin B12 + BH_4^- without particulate metals were applied for the dechlorination of CF, the selectivities to DCM were (25 ± 5) mol-% and (40 ± 5) mol-%, respectively. The DCM remained more-or-less as a dead-end by-product. Therefore, one can conclude that there is a synergy between CBRS and vitamin B12, which is beneficial for the

dechlorination reactions (1) to (6) in FIGURE 2. The reductive dehalogenation of HOCs by vitamin B12 in the presence of reducing agents such as titanium (III) acetate and $NaBH_4$ is considered to involve two-electron transfer processes to the electrophilic carbon by the super-reduced form of vitamin B12 (Co^{1+}, assigned as B12s) (Burris et al., 1996; Huang et al., 2013; Huang et al., 2015; Shey and van der Donk, 2000; Shimakoshi et al., 2005). In the presence of CBRS, vitamin B12 acts as an electron mediator (Huang et al., 2013; Huang et al., 2015). Hence, two-electron transfer processes could be responsible for the accelerated dechlorination of CF and DCM by CBRS + vitamin B12. For CBRS + vitamin B12, the ratio of the specific metal activities for dechlorination of CF and DCM is $A_{m,CF}/A_{m,DCM} = 17$, which is comparable to $A_{Ag,CF}/A_{Ag,DCM} = 9.5$. The advantage of CBRS + vitamin B12 compared to Ag-containing catalysts is seen in its subsequent ability to transform MCM. Therefore, CBRS + vitamin B12 can be considered as an optimal combination for the dechlorination of CF in water. However, vitamin B12 as a fine chemical (cost is about USD 96/g) (Vitamin B12, 2021) is even more expensive than Pd. Thus, it may not be a viable co-catalyst with Cu in full-scale water treatment applications.

Dechlorination of CF at Cu and Cu-modified surfaces under borohydride-free conditions

It was demonstrated earlier that for Pd + H_2 and Pd + BH_4^-, product selectivity patterns were independent of the type of the primary reductant used. Since under ambient conditions Cu is unable to activate molecular hydrogen into active H*, it was combined with zero-valent iron (ZVI) as a source of activated hydrogen in order to allow nascent hydrogen to interact with the Cu surface. ZVI-containing composite colloids (Carbo-Iron® colloids) without and with sulfide doping for corrosion protection (CIC and S/CIC, respectively) were applied as sorption-active reagents and then modified by 2 wt-% Cu to obtain Cu/CIC and Cu/S/CIC. CIC consists of colloidal activated carbon with embedded nZVI structures (Bleyl et al., 2012; Mackenzie et al., 2012). Further

modifications of Cu/CIC and Cu/S/CIC were made with Pd, Ni, and Ag. The selectivity patterns during the dechlorination of CF using CIC, S/CIC, and their metal-amended derivatives are presented in TABLE 3. The analyses of educt and chlorinated by-products were determined by solvent extraction, while k_{obs} values were calculated from methane formation (further details in SI 2). CF dechlorination by CIC and S/CIC combines adsorptions onto the activated carbon (AC) carriers with electron transfer from the embedded nZVI reagent. As shown in TABLE 3, similar selectivity patterns were observed for both CIC and S/CIC. The product patterns were similar to freely suspended nZVI (data in TABLE 2). Therefore, the adsorption of CF onto the AC carrier and sulfidation of the embedded ZVI has no marked effects on the product selectivity patterns.

TABLE 3. Selectivity patterns during the dechlorination of CF in water using CIC, S/CIC and their metal-modified forms ($c_{0,CF}$ = 10 mg/L; pH = 8; $c_{CIC} = c_{S/CIC} = c_{Cu/CIC} = c_{1\ wt\text{-}\%\ Ni/Cu/CIC} = c_{1\ wt\text{-}\%\ Pd/Cu/CIC} = c_{0.02\ wt\text{-}\%\ Ag/Cu/CIC} = c_{0.2\ wt\text{-}\%\ Ag/Cu/CIC} = c_{1\ wt\text{-}\%\ Ag/Cu/CIC}$ = 300 mg/L).

Reduction system		$n_{product} / n_{converted\ CF} \times 100$ (%)			k_{obs} (1/min)
		CH_4	**DCM**	**MCM**	
Unmodified sorption-active reagents	CIC	45 ± 4	40 ± 4	10 ± 2	0.0040 ± 0.0005
	S/CIC	50 ± 2	45 ± 2	3 ± 1	0.005 ± 0.001
Cu-modified reagents	Cu/CIC	82 ± 2	14 ± 2	1 ± 0.3	0.013 ± 0.003
	Cu/S/CIC	65 ± 5	25 ± 3	5 ± 2	0.008 ± 0.002
Cu-modified reagents amended with hydrogen-activating metals	1 wt-% Ni/Cu/CIC	70 ± 2	13 ± 2	2 ± 1	0.0020 ± 0.0002
	1 wt-% Pd/Cu/CIC	75 ± 2	15 ± 3	1 ± 0.2	0.0030 ± 0.0005
Cu-modified reagents amended with Ag	0.02 wt-% Ag/Cu/CIC	88 ± 2	5 ± 1	6 ± 2	0.045 ± 0.005
	0.2 wt-% Ag/Cu/CIC	90 ± 2	4 ± 1	5 ± 1	0.075 ± 0.005
	1 wt-% Ag/Cu/CIC	92 ± 2	2 ± 1	5 ± 1	0.30 ± 0.05
	1 wt-% Ag/Cu/S/CIC	86 ± 2	5 ± 1	6 ± 1	0.0040 ± 0.0005

ZVI was the only reductant here. No borohydride was used.

The deposition of metallic Cu onto nZVI leads to the formation of galvanic elements. In the process of ZVI corrosion ($Fe^0 + 2H_2O \rightarrow Fe^{2+} + H_2 + 2OH^-$), adsorbed H^+ ions can gain electrons and are then transformed to nascent hydrogen H* on the surface of Cu. Dechlorination of CF then takes place at the Cu surface, driven by active H*. Similar product patterns for Cu/CIC (data in TABLE 3) and CBRS (data in TABLE 2) indicate that the source of active H* for Cu, from ZVI or BH_4^-, has no marked effect on the product patterns. The presence of sulfide in Cu/S/CIC led to an increase in DCM selectivity by a factor of 2 compared to Cu/CIC. This is similar to CBRS in the presence of Na_2S. Hence, the presence of sulfur species favors stepwise hydrogenolysis, leading to higher DCM selectivity. Modification of Cu/CIC with Pd and Ni had no marked effects on the selectivity towards DCM. Ag deposition onto Cu/CIC has a selectivity effect similar to that described for Ag + BH_4^- and Ag + CBRS. The selectivities were independent of the extent of Ag loading onto Cu/CIC (between 0.02 and 1 wt-%). Thus, Ag is only required in small amounts.

Electrochemical dechlorination of CF at Cu and Cu-modified surfaces

The electron pressure for Cu catalysts provided by ZVI (in Cu/CIC and its modified forms) can also be provided electrochemically by the application of an external electric potential. Cu-based working electrodes were used for the dechlorination of CF. The electrochemical setup for dechlorination of CF using a Cu electrode is presented in FIGURE SI 6. Since metallic Cu acts as a catalyst, the experimental conditions were adjusted such that Cu existed in its oxidation state 0 (FIGURES SI 7 and SI 8). Cu^0 on activated carbon felt (ACF) as conductive support material was prepared and applied at potentials where water electrolysis was minimized (FIGURE SI 10).

Baseline experiments were performed in the absence of applied potential (open-circuit system). Control experiments were carried out with a Cu electrode maintained at -0.5 and -0.8 V versus Ag/AgCl, whereby the electrolyte and headspace were purged with H_2. For further comparison, electrochemical dechlorination of CF was carried out at -1.1 V using a Cu-mesh electrode. The results for the dechlorination of CF at Cu and Cu/ACF electrodes are presented in TABLE 4. In control experiments, CF remained stable for 12 h. Hence the activation of dissolved H_2 at the Cu electrode to form active H* due to the applied potential (-0.5 and -0.8 V) did not occur. As shown in TABLE 4, applied potential has no marked effect on product selectivity patterns. From a mechanistic point of view, these results suggest that the electron-transfer steps to CF adsorbed at Cu and Cu/ACF surfaces are not driven by the potential of free electrons (in the conduction band) but more likely by reactive hydrogen species from BH_4^- (possibly hydride species).

TABLE 4. Product patterns during the dechlorination of CF in water using Cu- and Cu/ACF-electrodes with external electric potentials and with/without $NaBH_4$ ($m_{\text{Cu-electrode}}$ = 370 mg; $m_{0.5\ \text{wt-\% Cu/AC}}$ = 6.3 mg; $c_{0,\text{CF}}$ = 5 mg/L; $c_{0,\text{NaBH4}}$ = 300 mg/L; pH_0 = 7; $V_{\text{electrolyte}}$ = 400 mL of 0.1 M Na_2SO_4; $V_{\text{headspace}}$ = 100 mL).

Electrode type and reaction conditions	$n_{\text{product}} / n_{\text{transferred CF}} \times 100$ **(%)**			**Cl^- yield (mol-%)**
	CH_4	DCM	MCM	
Cu electrode + $NaBH_4$ (open circuit system)	82 ± 2	14 ± 2	5 ± 1	84 ± 3
-1.1 V[a] + Cu electrode (electrochemical dechlorination reaction)	82 ± 2	13 ± 2	2 ± 1	85 ± 2
-0.8 V[a] + Cu electrode + $NaBH_4$	84 ± 3	11 ± 3	3 ± 1	84 ± 2
-1.0 V[a] + Cu electrode + $NaBH_4$	85 ± 2	12 ± 3	4 ± 2	85 ± 3
-0.8 V[a] + Cu/ACF electrode + $NaBH_4$	85 ± 2	10 ± 2	3 ± 1	88 ± 2

[a] Applied potentials of the working electrodes were measured against Ag/AgCl.
Product selectivities were determined at 30-40 % CF conversion.
The chloride yields were determined at CF conversions of ≥ 95 %.
For all CF dechlorination reactions, the sum of C_2H_4 and C_2H_6 accounts for 1-2 mol-% measured at CF conversion ≥ 95 %.

Surprisingly, the electrochemical dechlorination reaction (due to electrons in the conduction band) had similar selectivity patterns to the borohydride-assisted reaction. Similar selectivity patterns have also been reported elsewhere for the electrochemical dechlorination of CF in water at a graphite electrode with cathodic potentials in the range -0.75 to -1.3 V versus Ag/AgCl (Battke, 2006). Comparison between the current results and those of Battke (2006) show that a higher cathodic potential has no marked effect on initial product patterns.

The formation of similar product patterns in the presence of various primary reductants (i.e. $NaBH_4$, H_2, ZVI, and external electric potentials) for Cu, Ag, and Pd catalysts is a significant finding from the mechanistic point of view. Apparently, the primary reductants generate similar reactive species (active H^* or electrons) which are responsible for the initial surface-mediated (catalytic) dechlorination steps.

Dehalogenation of CCl_4, $CFCl_3$, $CBrCl_3$, CCl_3–CH_3, 1,1-DCA and DCM using CBRS

Another objective of this study was to determine how substance structure affects product selectivity patterns. Substances similar to CF but different in their substitution patterns were selected. The dehalogenation of these substances by CBRS was carried out under identical reaction conditions to CF. The product selectivity patterns during the dehalogenation of CCl_4, $CFCl_3$, and $CBrCl_3$ and their first daughter products are presented in FIGURE 4. Further details are shown in FIGURES SI 11-13.

As can be seen in FIGURE 4 (a), the immediate daughter products from the reduction of CCl_4 and $CFCl_3$ were CF and $CHCl_2F$; they accounted for 52-72 mol-% of the educt converted. For $CBrCl_3$, the selectivities to CF and DCM were 15 and 40 mol-%, respectively. For CCl_4 and $CBrCl_3$, selectivities towards CH_4 were 16 and 35 mol-%, respectively. CH_4 and F^- were not

detected during the dehalogenation of $CFCl_3$. Hence, CBRS fails to cleave C–F bonds. CF and $CHCl_2F$ as intermediates were further transformed (FIGURE 4 (b)) by the subsequent generation of MCM, DCM, CH_4, CH_2ClF, and CH_3–F. MCM, DCM, CH_2ClF, and CH_3–F remained as dead-end by-products under the chosen reaction conditions (c_{Cu} = 0.2-2 mg/L). Hence, by replacing the chloroform's H-substituent with F, Cl, and Br, hydrogenolysis becomes dominant over α-elimination. This is plausible because the preferred elimination of HCl is not possible from these molecules. In addition, electron-withdrawing and steric effects at the electrophilic carbon might be significant.

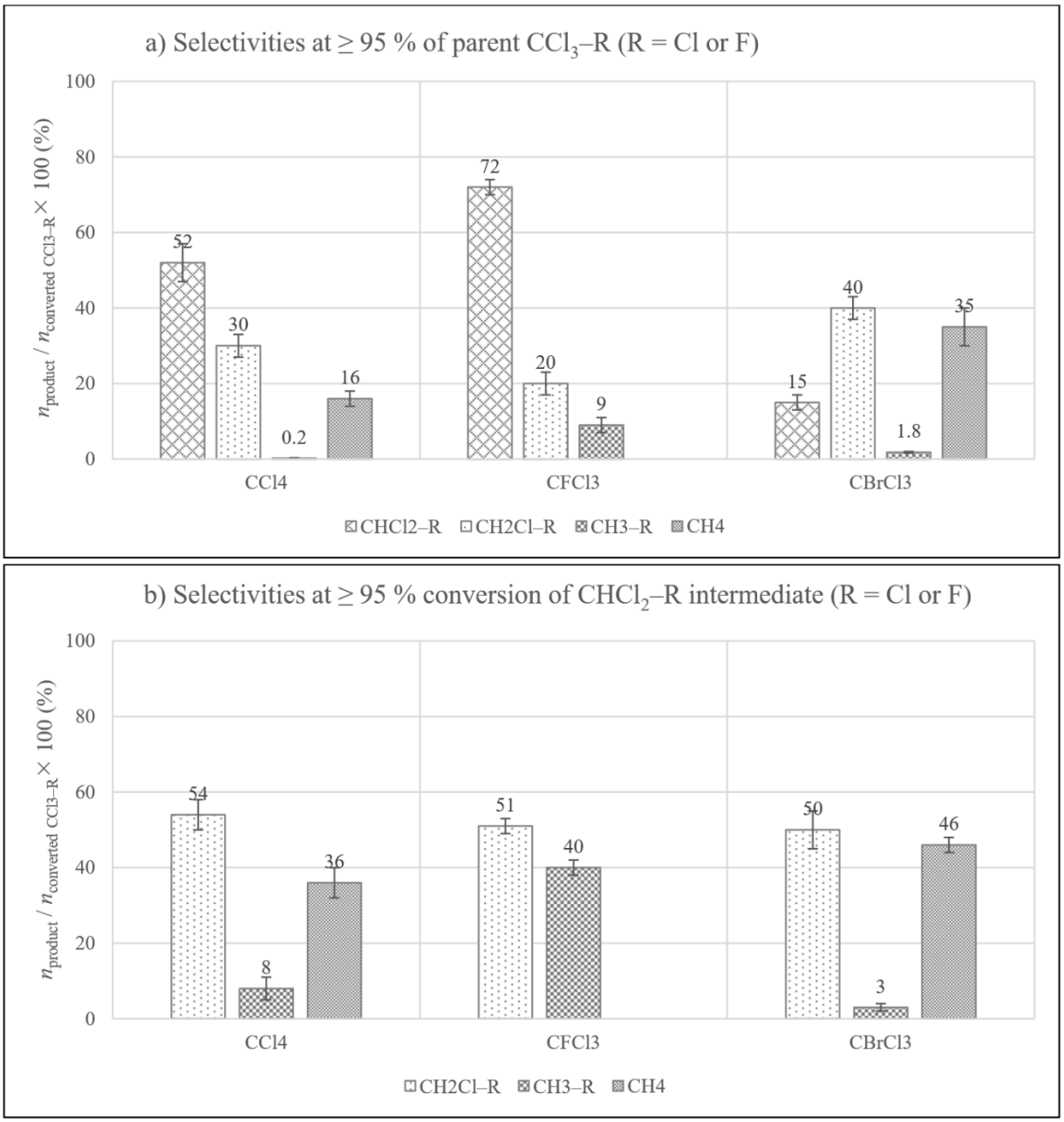

FIGURE 4. Product selectivity patterns during the dehalogenation of CCl_4, $CFCl_3$, and $CBrCl_3$ by CBRS. a) Selectivities at ≥ 95 % conversion of the parent CCl_3–R compound, and b) selectivities at ≥ 95 % conversion of the immediate $CHCl_2$–R intermediate (c_{Cu} = 0.2-2 mg/L; $c_{0,educt}$ = 20 mg/L; $c_{0,NaBH4}$ = 300 mg/L; pH = 10).

In order to investigate steric effects, dechlorination of CCl_3-CH_3 (1,1,1-TCA), where the chloroform's H-substituent is replaced by the bulkier methyl group, was performed. The resulting selectivity patterns are shown in FIGURE 5. Further details are shown in FIGURE SI 14.

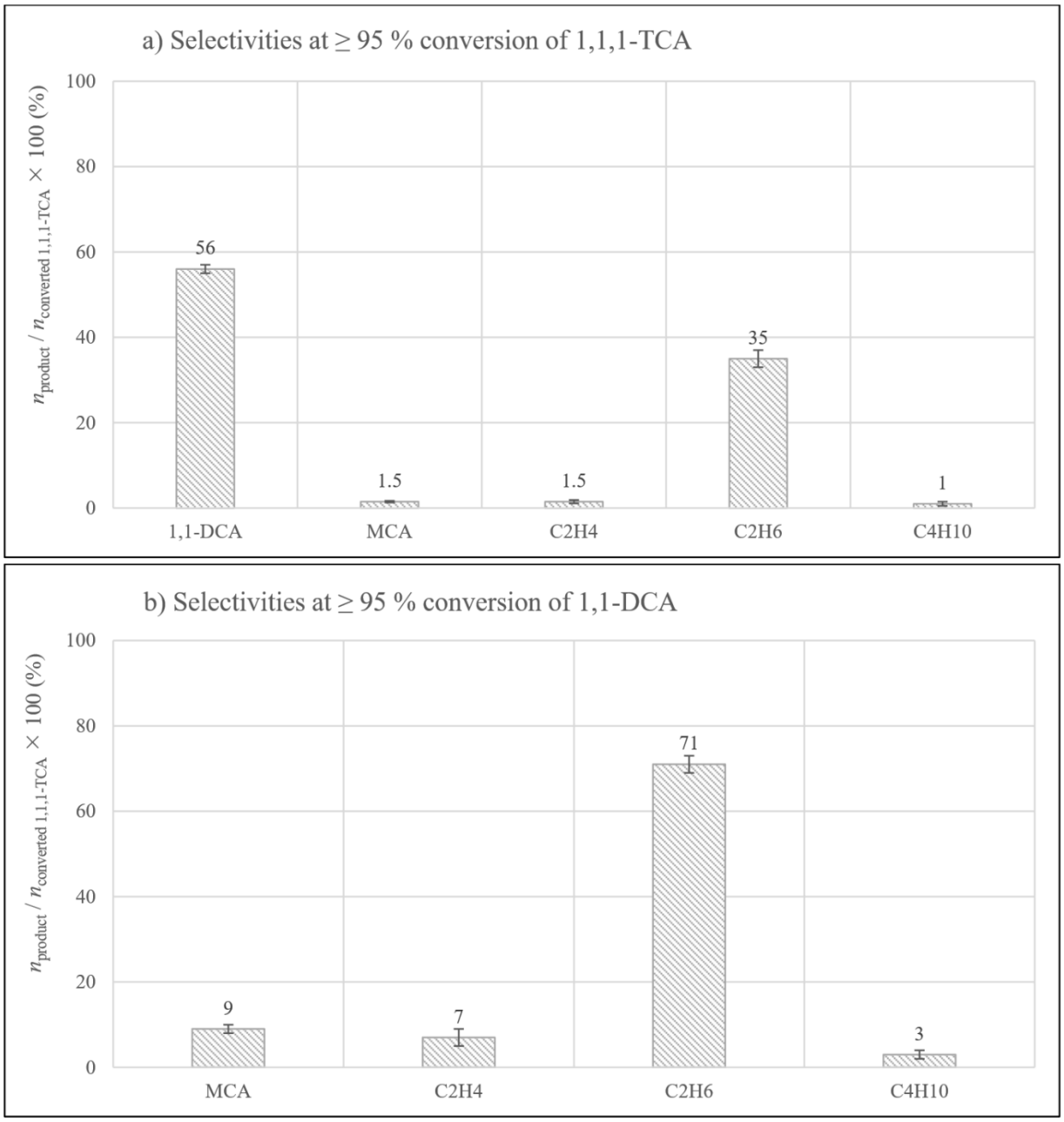

FIGURE 5. Product selectivity patterns during the dechlorination of 1,1,1-TCA by CBRS. a) Selectivities at ≥ 95 % conversion of 1,1,1-TCA, and b) selectivities at ≥ 95 % conversion of the 1,1-DCA intermediate (c_{Cu} = 1 mg/L; $c_{0,1,1,1\text{-}TCA}$ = 20 mg/L; $c_{0,NaBH4}$ = 300 mg/L; pH = 10).

As can be seen in FIGURE 5 (a), 1,1-DCA with $S_{1,1\text{-}DCA}$ = (56 ± 2) mol-% was the major chlorinated intermediate, while C_2H_6 accounted for only (35 ± 2) mol-% of the 1,1,1-TCA converted. This implied that hydrogenolysis was preferred over α-elimination. Further

dechlorination of 1,1-DCA (FIGURE 5 (b)) led to increased amounts of MCA, C_2H_4, C_4H_{10}, and C_2H_6, i.e. 9, 7, 3, and 71 mol-%, respectively. MCA remained more-or-less as a dead-end by-product at the low catalyst concentration (c_{Cu} = 1 mg/L). However, with a high catalyst concentration of c_{Cu} = 100 mg/L, MCA was further dechlorinated. The specific Cu activity A_{Cu} for the dechlorination of MCA in water under ambient conditions was $A_{Cu,MCA}$ = (0.010 ± 0.005) L/(g·min).

For the CCl_3–R compounds with R = F, Cl, Br, and CH_3, similar initial product patterns were observed, indicating that the initial dehalogenation reaction at the Cu surfaces follows similar reduction steps. For $CFCl_3$ and CCl_4, F and Cl as substituents at the CCl_3-group have an electron-withdrawing effect on the carbon, making it more electrophilic, hence destabilizing C-centered radicals. In contrast, for 1,1,1-TCA, the methyl substituent has a radical stabilization effect. Nevertheless, all CCl_3–R compounds show similar initial product patterns regarding the first intermediates CF, $CHCl_2F$, and 1,1-DCA. This suggests that the electronic effects of the substituent play no significant role in the initial dehalogenation steps. In order to further whether initial selectivity patterns are influenced by steric effects, dechlorination of DCM and 1,1-DCA by CBRS were performed. The results are shown in FIGURE 6.

By replacement of one Cl-substituent in CF and 1,1,1-TCA, it can be seen from FIGURE 6 that the dechlorination of DCM and 1,1-DCA produces CH_4 and C_2H_6, respectively, as the major products. This indicates that the α-elimination reaction pathway was preferred in the dechlorination of DCM and 1,1-DCA. Both molecules can eliminate HCl.

FIGURE 6. Product selectivity patterns for the dechlorination of DCM and 1,1-DCA by CBRS (c_{Cu} = 50-100 mg/L; $c_{0,educt}$ = 10-20 mg/L; $c_{0,NaBH4}$ = 300 mg/L; pH = 10). Selectivity patterns determined at educt conversions ≥ 95 %.

Conclusions and Outlook

This study presents Cu in the presence of borohydride as a system that is more suitable than Pd + H_2 for the degradation of saturated aliphatic chloroorganic compounds in water. Cu is a much cheaper catalyst than Pd, but $NaBH_4$ is a more expensive reductant than H_2. In order to determine the application potential of CBRS, product selectivity patterns for the reduction of several CCl_3–R compounds were evaluated. For the dechlorination of $CHCl_3$ as a target pollutant, similar product selectivity patterns (ratio of CH_2Cl_2 : CH_4) were observed for several very different reduction systems. Therefore, the nature of reactive species (electrons or active H*) at the surfaces of Cu and Pd catalysts seems to play no significant role during the initial surface-mediated dechlorination steps. Initial product selectivity patterns were substance-specific rather than system-specific. Selectivity patterns depend on the substitution degree at the electrophilic carbon. For $CHCl_3$, CH_2Cl_2, and $CHCl_2$–CH_3, initial product selectivities were in preference of the fully

dechlorinated products, CH_4 and C_2H_6. For the highly substituted compounds, CCl_4, $CFCl_3$, $CBrCl_3$, and CCl_3–CH_3, initial product selectivities were in preference of the halogenated intermediates $CHCl_3$, CH_2Cl_2, $CHCl_2F$, and $CHCl_2$–CH_3. The availability of HCl at the reactive carbon during the dehalogenation of saturated aliphatic chloroalkanes in water favors the α-elimination pathway.

Although the formation of less-chlorinated by-products such as CH_2Cl_2 and CH_3Cl is inevitable during the dechlorination of CCl_4 and $CHCl_3$ by both CBRS and Pd + H_2, these by-products are further converted at reasonable rates only by CBRS. The optimum conditions for preventing accumulation of chlorinated by-products are $c_{Cu} \approx 100$ mg/L and $c_{0,NaBH4} \approx 300$ mg/L. A higher catalyst dose is acceptable for the cheaper catalyst, Cu instead of Pd. Instead of using a higher catalyst dose, other options for fast transformation of chlorinated by-products through a second dechlorination step include i) use of bimetallic Ag/Cu particles and ii) combination of CBRS with vitamin B12. In conclusion, CBRS is presented in this study as a robust reduction system that is superior to Pd + H_2 for the treatment of saturated aliphatic HOCs in water under controlled conditions. However, its application is limited to small-scale treatment plants where Cu recovery from the effluent can be achieved and the amounts of borohydride are manageable.

Acknowledgments

The author is grateful for the scholarship award from the Deutscher Akademischer Austauschdienst (DAAD) in cooperation with the Helmholtz Centre for Environmental Research (UFZ), Leipzig.

References

Angeles-Wedler D., Mackenzie K., Kopinke F.-D. Permanganate Oxidation of Sulfur Compounds to Prevent Poisoning of Pd Catalysts in Water Treatment Processes. Environmental Science & Technology 2008; 42: 5734-5739.

Angeles-Wedler D., Mackenzie K., Kopinke F.-D. Sulphide-Induced Deactivation of Pd/Al_2O_3 as Hydrodechlorination Catalyst and Its Oxidative Regeneration with Permanganate. Applied Catalysis B: Environmental 2009; 90: 613-617.

Balko B. A., Tratnyek P. G. Photoeffects on the Reduction of Carbon Tetrachloride by Zero-Valent Iron. The Journal of Physical Chemistry B 1998; 102: 1459-1465.

Battke J. Interaktion von Sorption und Reaktion bei der Dehalogenierung von Halogenorganischen Verbindungen in Wasser. Fakultät für Verfahrensund Systemtechnik. PhD. Otto-von-Guericke-Universität Magdeburg, UFZ-Umweltforschungszentrum Leipzig-Halle GmbH, 2006.

Benitez J. L., Del Angel G. Effect of Chlorine Released During Hydrodechlorination of Chlorobenzene over Pd, Pt and Rh Supported Catalysts. Reaction Kinetics and Catalysis Letters 2000; 70: 67-72.

Bleyl S., Kopinke F.-D., Mackenzie K. Carbo-Iron®—Synthesis and Stabilization of Fe(0)-Doped Colloidal Activated Carbon for *In Situ* Groundwater Treatment. Chemical Engineering Journal 2012; 191: 588-595.

Burris D. R., Delcomyn C. A., Smith M. H., Roberts A. L. Reductive Dechlorination of Tetrachloroethylene and Trichloroethylene Catalyzed by Vitamin B12 in Homogeneous and Heterogeneous Systems. Environmental Science & Technology 1996; 30: 3047-3052.

Copper Prices. Copper Prices - 45 Year Historical Chart. 2021; *https://www.macrotrends.net/1476/copper-prices-historical-chart-data*. Accessed April 21 2021

Danielsen K. M., Gland J. L., Hayes K. F. Influence of Amine Buffers on Carbon Tetrachloride Reductive Dechlorination by the Iron Oxide Magnetite. Environmental Science & Technology 2005; 39: 756-763.

Dekant W., Jean P., Arts J. Evaluation of the Carcinogenicity of Dichloromethane in Rats, Mice, Hamsters and Humans. Regulatory Toxicology and Pharmacology 2021; 120: 104858.

Dong H., Li L., Lu Y., Cheng Y., Wang Y., Ning Q., Wang B., Zhang L., Zeng G. Integration of Nanoscale Zero-Valent Iron and Functional Anaerobic Bacteria for Groundwater Remediation: A Review. Environment International 2019; 124: 265-277.

Elsner M., Haderlein S. B., Kellerhals T., Luzi S., Zwank L., Angst W., Schwarzenbach R. P. Mechanisms and Products of Surface-Mediated Reductive Dehalogenation of Carbon Tetrachloride by Fe(II) on Goethite. Environmental Science & Technology 2004; 38: 2058-2066.

Feng J., Lim T. T. Iron-Mediated Reduction Rates and Pathways of Halogenated Methanes with Nanoscale Pd/Fe: Analysis of Linear Free Energy Relationship. Chemosphere 2007; 66: 1765-74.

Fennelly J. P., Roberts A. L. Reaction of 1,1,1-Trichloroethane with Zero-Valent Metals and Bimetallic Reductants. Environmental Science & Technology 1998; 32: 1980-1988.

Han Y., Liu C., Horita J., Yan W. Trichloroethene Hydrodechlorination by Pd-Fe Bimetallic Nanoparticles: Solute-Induced Catalyst Deactivation Analyzed by Carbon Isotope Fractionation. Applied Catalysis B: Environmental 2016; 188: 77-86.

Hildebrand H., Mackenzie K., Kopinke F.-D. Highly Active Pd-on-Magnetite Nanocatalysts for Aqueous Phase Hydrodechlorination Reactions. Environmental Science & Technology 2009; 43: 3254-3259.

Huang C.-C., Lo S.-L., Lien H.-L. Zero-Valent Copper Nanoparticles for Effective Dechlorination of Dichloromethane Using Sodium Borohydride as a Reductant. Chemical Engineering Journal 2012; 203: 95-100.

Huang C.-C., Lo S.-L., Lien H.-L. Synergistic Effect of Zero-Valent Copper Nanoparticles on Dichloromethane Degradation by Vitamin B12 under Reducing Condition. Chemical Engineering Journal 2013; 219: 311–318.

Huang C.-C., Lo S.-L., Lien H.-L. Vitamin B12-Mediated Hydrodechlorination of Dichloromethane by Bimetallic Cu/Al Particles. Chemical Engineering Journal 2015; 273: 413-420.

Huang C.-C., Lo S.-L., Tsai S.-M., Lien H.-L. Catalytic Hydrodechlorination of 1,2-Dichloroethane Using Copper Nanoparticles under Reduction Conditions of Sodium Borohydride. Journal of Environmental Monitoring 2011; 13: 2406-2412.

Li T., Farrell J. Reductive Dechlorination of Trichloroethene and Carbon Tetrachloride Using Iron and Palladized-Iron Cathodes. Environmental Science & Technology 2000; 34: 173-179.

Lim T.-T., Zhu B.-W. Effects of Anions on the Kinetics and Reactivity of Nanoscale Pd/Fe in Trichlorobenzene Dechlorination. Chemosphere 2008; 73: 1471-1477.

Liu B. H., Li Z. P. A Review: Hydrogen Generation from Borohydride Hydrolysis Reaction. Journal of Power Sources 2009; 187: 527-534.

Lowry G. V., Reinhard M. Hydrodehalogenation of 1- to 3-Carbon Halogenated Organic Compounds in Water Using a Palladium Catalyst and Hydrogen Gas. Environmental Science & Technology 1999; 33: 1905-1910.

Lowry G. V., Reinhard M. Pd-Catalyzed TCE Dechlorination in Groundwater: Solute Effects, Biological Control, and Oxidative Catalyst Regeneration. Environmental Science & Technology 2000; 34: 3217-3223.

Mackenzie K., Bleyl S., Georgi A., Kopinke F. D. Carbo-Iron - an Fe/AC Composite - as Alternative to Nano-Iron for Groundwater Treatment. Water Research 2012; 46: 3817-26.

Mackenzie K., Frenzel H., Kopinke F.-D. Hydrodehalogenation of Halogenated Hydrocarbons in Water with Pd Catalysts: Reaction Rates and Surface Competition. Applied Catalysis B: Environmental 2006; 63: 161-167.

McCormick M. Biotic and Abiotic Transformations of Alkyl Halides in Iron Reducing Environments. Health and Environmental Sciences. PhD. University of Michigan, Ann Arbor, Michigan, USA, 2002, pp. 281.

McCormick M. L., Adriaens P. Carbon Tetrachloride Transformation on the Surface of Nanoscale Biogenic Magnetite Particles. Environmental Science & Technology 2004; 38: 1045-1053.

Ordóñez S., Sastre H., Díez F. V. Hydrodechlorination of Aliphatic Organochlorinated Compounds over Commercial Hydrogenation Catalysts. Applied Catalysis B: Environmental 2000; 25: 49-58.

Palladium Prices. Palladium Prices - Interactive Historical Chart. 2021; *https://www.macrotrends.net/2542/palladium-prices-historical-chart-data*. Accessed April 21 2021

Retnamma R., Novais A. Q., Rangel C. M. Kinetics of Hydrolysis of Sodium Borohydride for Hydrogen Production in Fuel Cell Applications: A Review. International Journal of Hydrogen Energy 2011; 36: 9772-9790.

Schlosser P. M., Bale A. S., Gibbons C. F., Wilkins A., Cooper G. S. Human Health Effects of Dichloromethane: Key Findings and Scientific Issues. Environmental Health Perspectives 2015; 123: 114-119.

Shey J., van der Donk W. A. Mechanistic Studies on the Vitamin B12-Catalyzed Dechlorination of Chlorinated Alkenes. Journal of the American Chemical Society 2000; 122: 12403-12404.

Shimakoshi H., Maeyama Y., Kaieda T., Matsuo T., Matsui E., Naruta Y., Hisaeda Y. Hydrophobic Vitamin B12. Part 20: Supernucleophilicity of Co(I) Heptamethyl Cobyrinate toward Various Organic Halides. Bulletin of the Chemical Society of Japan 2005; 78: 859-863.

Silver Prices. Silver Prices - 100 Year Historical Chart. 2021; *https://www.macrotrends.net/1470/historical-silver-prices-100-year-chart?q=*. Accessed April 23 2021

Song H., Carraway E. Reduction of Chlorinated Methanes by Nano-Sized Zero-Valent Iron. Kinetics, Pathways, and Effect of Reaction Conditions. Environmental Engineering Science 2006; 23: 272-284.

Song H., Carraway E. R. Reduction of Chlorinated Ethanes by Nanosized Zero-Valent Iron: Kinetics, Pathways, and Effects of Reaction Conditions. Environmental Science & Technology 2005; 39: 6237-45.

Urbano F. J., Marinas J. M. Hydrogenolysis of Organohalogen Compounds over Palladium Supported Catalysts. Journal of Molecular Catalysis A: Chemical 2001; 173: 329-345.

Velázquez J., Leekumjorn S., Nguyen Q., Fang Y. L., Heck K., Hopkins G., Reinhard M., Wong M. Chloroform Hydrodechlorination Behavior of Alumina-Supported Pd and PdAu Catalysts. AIChE Journal 2013; 59: 4474-4482.

Vitamin B12. Vitamin B12. 2021; *https://www.chemicalbook.com/Price/Vitamin-B12.htm*. Accessed July 27 2021

Vogel M., Nijenhuis I., Lloyd J., Boothman C., Pöritz M., Mackenzie K. Combined Chemical and Microbiological Degradation of Tetrachloroethene During the Application of Carbo-Iron at a Contaminated Field Site. Science of The Total Environment 2018; 628-629: 1027-1036.

Wade R. C. Catalyzed Reduction of Organofunctional Groups with Sodium Borohydride. Journal of Molecular Catalysis 1983; 18: 273-297.

Wang X., Chen C., Chang Y., Liu H. Dechlorination of Chlorinated Methanes by Pd/Fe Bimetallic Nanoparticles. Journal of Hazardous Materials 2009; 161: 815-823.